

PAPER • OPEN ACCESS

An Active Compliance Control for A Robotic Wound Closure System

To cite this article: Edward H. Currie *et al* 2020 *IOP Conf. Ser.: Mater. Sci. Eng.* **922** 012007

View the [article online](#) for updates and enhancements.

You may also like

- [POPX2 phosphatase enhances topographical contact guidance for cell morphology and migration](#)
Sharvari R Sathe, Deepak Jain, Cheng-Gee Koh et al.
- [Modeling closure of circular wounds through coordinated collective motion](#)
David S Li, Juliane Zimmermann and Herbert Levine
- [Nanocrystalline cellulose–hyaluronic acid composite enriched with GM-CSF loaded chitosan nanoparticles for enhanced wound healing](#)
Nakisa Karimi Dehkordi, Mohsen Minaiyan, Ardeshir Talebi et al.



ECS
The
Electrochemical
Society
Advancing solid state &
electrochemical science & technology

DISCOVER
how sustainability
intersects with
electrochemistry & solid
state science research

An Active Compliance Control for A Robotic Wound Closure System

Edward H. Currie¹, Y. M Zhao¹, Louis Kavoussi², Sina Y. Rabbany¹

¹DeMatteis School of Engineering and Applied Science, Hofstra University, Hempstead, New York

²Department of Urology, Long Island Jewish Medical Centre

Abstract. Most approaches to medical robotic compliance control rely upon forces, or torques, exerted on the mechanical arm links. The majority of robotic arms allow only position control, and orientation, of the end-effector. This paper uses a soft control technique to develop a position-correction, impedance method that leads to similar responses to the contact environment for simulation. The system is applied to control the contact force between a fixture and the skin in a robotic, vision-controlled, wound closure system. The experimental results show that the algorithm is successful in controlling contact force in fixture placement on different skin models.

1. Introduction

The importance of interaction control has been a subject of study in the last decades, resulting in advances in power electronics, computational power, and sensors [1]. The challenge with this approach is the contact's nonlinear behaviour, where classical techniques fall short [2]. Alternative approaches dealing with the transition from unconstrained-to-constrained motion have been studied including impedance control, has been proposed by Hogan [3]. This latter technique has received significant attention in recent years, as impedance control is has the potential to achieve the desired mechanical interaction within uncertain environments [4]. In the present context, impedance refers to the dynamic relation between the motion variables of a manipulator and the contact force. The primary benefit of impedance control is that it provides an effective way to simultaneously control the motion and contact force. This is paramount developing safe autonomous human-robot interactions. The implementation methods can be categorized into two main classes: a software-based approach [5-6] and a hardware-based approach [7-8]. Although many innovative applications use this technique, it is not a trivial task to achieve, therefore it is worthwhile to its corresponding algorithmic implementation.

Manual surgical procedures such as suturing can exhibit significant variations in technique and effectiveness due to the procedure's dependence on an individual manual dexterity. In order to optimize as well as standardize outcomes, interest in robotic wound closure systems has evolved. The concept of impedance control was introduced into medical robotics research and has gradually resulted in many specific implementation strategies [9]. Moreover, medical applications need to interact with the environment in such a compliant way that superior dexterity, over that of humans, is provided to the end-effector of a robotic arm. This paper presents a method to control the contact force between a fixture and the skin in a robotic wound closure system using a position-correction, impedance control, strategy organized as follows: Section 2 gives some essential explanations about the concept of impedance control. Position-correction methods to implement impedance control are introduced in



Section 3. The skin model, the interaction of fixture and wound skin, and a schematic diagram of position-correction impedance control are described in Section 4. The simulation and experimental results are presented in Section 5. Section 6 presents conclusions

2. Impedance control implementation

2.1. Impedance control dynamic equation.

Impedance control may be understood as a complex scheme behaving like a second-order, dynamic system. Figure 1 displays a simplified model of a mechanical assembly, with inertial, spring and damper components. Equation (1) describes the model's dynamics in the Laplace domain, where $X(s)$ is the displacement of the Tool Centre Point (TCP), $F_{int}(s)$ is the interaction force with the environment, M is the inertial component, B is the energy dissipation term from the viscous damper, and K is the stiffness of the equivalent system.

$$X(s) = \frac{F_{int}(s)}{Ms^2 + Bs + K} = G(s)F_{int}(s) \quad (1)$$

2.2. Solution by discrete-time convolution.

Discrete-time convolution is an operation on two discrete-time signals defined by the integral

$$(f * g)(n) = \sum_{k=-\infty}^{\infty} f(k)g(n - k) \quad (2)$$

for all signals f, g defined on Z . The above operation has proven to be particularly useful in the study of linear, time-invariant systems. In order to see this, consider a linear time-invariant system H with a unit impulse response h . Given a system input signal x , we would like to compute the system's output signal $H(x)$. First, we note that the input can be expressed as the convolution:

$$x(n) = \sum_{k=-\infty}^{\infty} x(k)\delta(n - k) \quad (3)$$

Where $\delta(n - k)$ is unit sample sequence or unit impulse or Kronecker delta function, i.e.,

$$\delta(n - k) = \begin{cases} 1 & n = k \\ 0 & n \neq k \end{cases} \quad (4)$$

Since $H\delta(n - k)$ is the shifted unit impulse response $h(n - k)$, this gives the result

$$Hx(n) = \sum_{k=-\infty}^{\infty} x(k)h(n - k) = (x * h)(n) \quad (5)$$

Hence, convolution has been defined such that the output of a linear, time-invariant system is given by the convolution of the system input with the system's unit impulse response.

3. Skin modelling and contact interaction

3.1. *Skin modelling.* Most materials can be considered linear if the strain and stress remain small. If the strain remains linear, the mechanical behaviour is considered linear. Such linear behaviours can then modelled by parallel and/or a serial combination of linear springs (i.e., springs with a constant stiffness coefficient) and linear dashpots (with a constant damping coefficient), e.g., linear viscoelastic bodies such as a generalized Kelvin-Voigt body or a generalized Maxwell body as presented in Figure 1 (a). Figure 1 (b) shows the interaction between the skin and the end-effector.

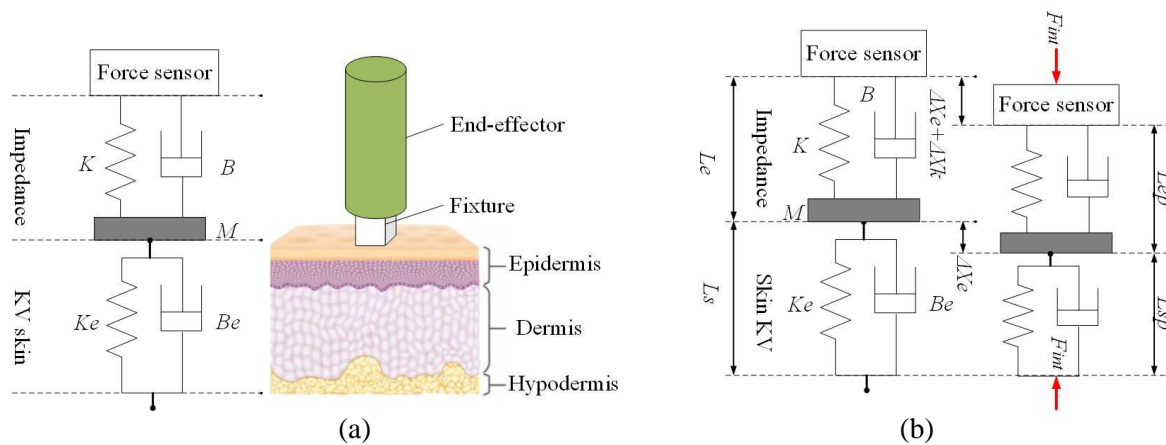


Figure 1. Skin modelling and contact impedance control dynamic model: (a) M - B - K impedance parameters; K_e - B_e skin model parameters, (b) Representing interaction analysis of skin and robot end-effector with contact force $F_{int}(t)$.

3.2. *Schematic diagram.* The control schematic diagram of position-correction impedance control is illustrated in figure 2.

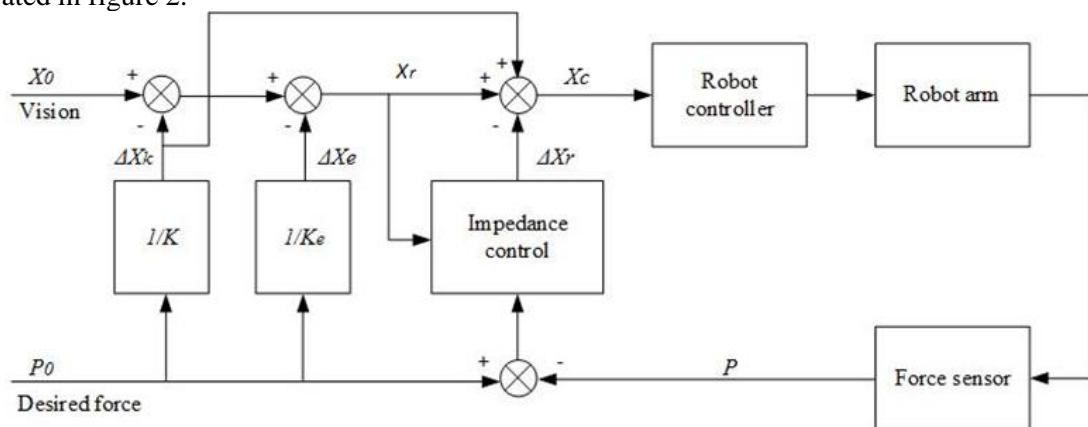


Figure 2. Diagram of position-based impedance control for the force between skin and robot arm

The correction to the robot's position, X_c , is the input to the robot controller in Figure 2. P_0 is the desired contact force and X_0 is the desired position of the fixture on the skin's surface, which is determined by a vision-guiding system.

4. Simulation and experiment results

4.1. *Experimental setup and e parameters.* The simulations and experiments validated the robotic arm position-correction impedance control strategy. The simulations were carried out in a Simulink environment (MATLAB 2018a). The experiments were performed on the robotic, vision-control wound closure system shown in Figure 3. The robotic, vision-control wound system included a Mitsubishi RV-2SDB robotic arm, fixture applicator, force sensor installed inside fixture applicator, wound model, stereo camera, and a laser pattern projector. For each task, the

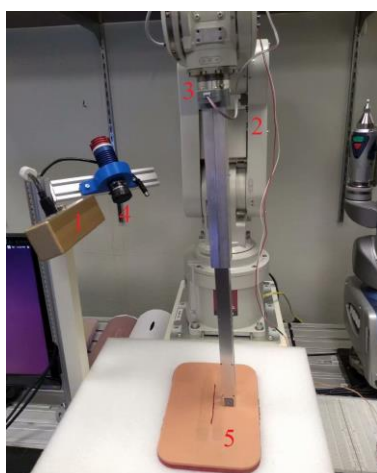


Figure 3. System configuration:
 1 - Stereo camera, 2 - Robotic arm,
 3 - Force sensor,
 4 - Laser projector,
 5 - Wound surface.

impedance parameters used were $M = 10 \text{ kg}$, $B = 18 \text{ N.s/m}$, and $K = 25 \text{ N/m}$.

4.2. Validation of contact force

Three skin models were studied for tracking the desired force trajectory using the proposed approach. The skin model parameters are list in Table 1.

Table 1. Skin model parameters.

Skin model	Parameters	
	$Be \text{ (N.s/m)}$	$Ke \text{ (N/m)}$
A	0.01	10
B	26	625
C	11	576

Determination of the unit impulse response for a discrete-time $h(k)$ is illustrated in figure 4. To prevent the overshoot of the response in fixture

placement on the skin’s surface, the impedance of the robotic arm functions as a second-order linear system with critical damping which provides the quickest approach to zero amplitude for a damped oscillator. The robot’s end-effector critical damping coefficient is given by: $B = 2 \cdot \sqrt{MK}$

If $M = 100 \text{ (kg)}$, $K = 100 \text{ (N/m)}$, then $B = 200 \text{ (N.s/m)}$. A unit impulse was used for the position-correction impedance control of the robot end-effector and is shown in figure 4 (a). The response to the unit impulse for a discrete-time $h(k)$ of the robotic arm in critical damping is shown in figure 4 (b).

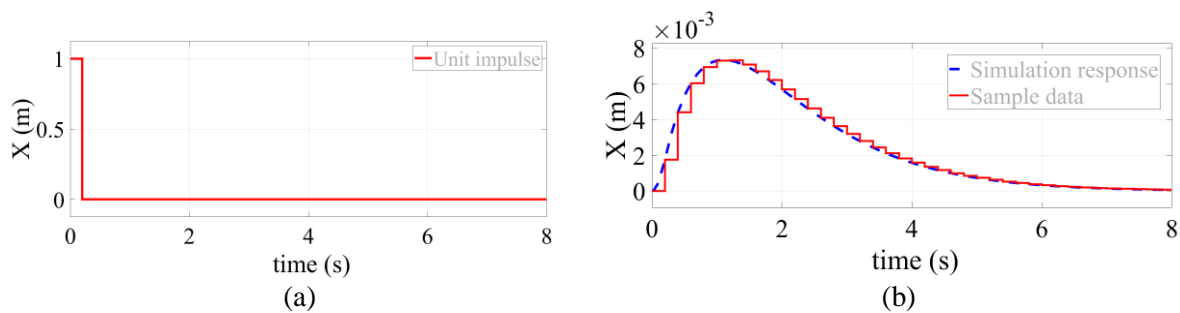
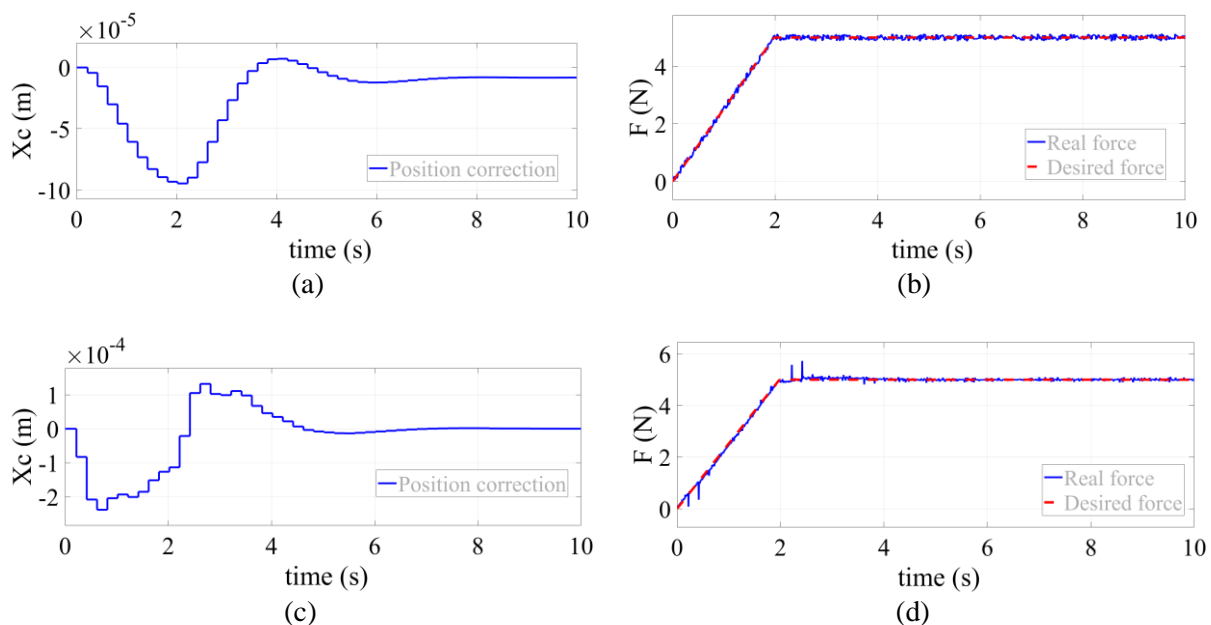


Figure 4. A unit impulse was used for position-correction impedance control and the response to a unit impulse for a discrete-time $h(k)$ of the robotic arm in critical damping.



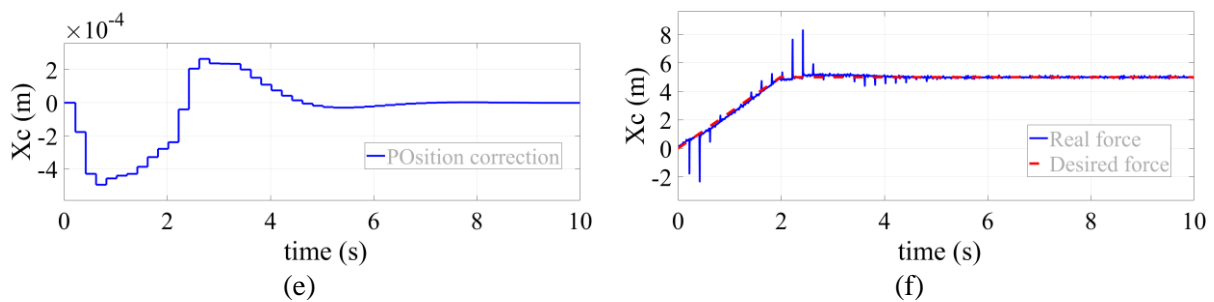


Figure 5. Experimental results for contact force tracking by position-correction impedance control: (a) Correction of robot end-effector of case A, (b) Contact force tracking of case A, (c) Correction of robot end-effector of case B, (d) Contact force tracking of case B, (e) Correction of robot end-effector of case C, (f) Contact force tracking of case C.

The experimental results are shown in figure 5. The corrections of the robot end-effector position are plotted in figure 5 (a), (c), and (e), respectively. Contact force tracking of the desired force trajectory is given in figure 8 (b), (d), and (f), respectively. The results demonstrate that the proposed position-correction impedance control can accurately track the contact force between the fixture and the skin surface. It can also track the reference contact force when the parameters of the skin model change. This implies that position-based impedance can be used for different skin models without changing the control parameters. The tracking errors for the reference force trajectory were measured and the errors evaluated in terms of the average errors (AEs) and standard deviation (SD), in the X-direction. The errors were computed, and the results are listed in Table 2.

Table 2. Formatting sections, subsections and subsubsections.

Case	Tracking error	
	AEs (N)	SD (N)
A	0.011	0.156
B	0.046	0.026
C	0.034	0.032

Table 2 shows that the softer the skin becomes, the smaller the AEs in X. It is also demonstrated that the proposed method can track the contact force between the fixture and the skin surface with 0.34 (N) and AEs within 3 (sec).

5. Conclusions

A contact force, tracking method based on the position-correction approach is proposed in this paper. The simulation and experimental results of contact force tracking on the skin models with different parameters or on different part of body was studied utilizing a robotic, vision-controlled, wound closure system. The results show that the proposed method, based on a position-correction of the robot end-effector, can accurately track the desired contact force trajectories between the end-effector and the skin models that have different parameters.

6. References

- [1] L. Villani and J. de Schutter, *Force Control*, in *Springer Handbook of Robotics*, B. Siciliano and O. Khatib, Eds. Berlin, Heidelberg: Springer Berlin Heidelberg, 2008, pp. 161184.
- [2] N. Hogan, "Adaptive Control of Mechanical Impedance by Coactivation of Antagonist Muscles," *IEEE Transactions on Automatic Control*, vol. 29, pp. 681-690, Aug. 1984.
- [3] N. Hogan, "Impedance Control: An approach to manipulation: Parts III," *J. Dyn. Syst. Meas. Control. Trans. ASME*, vol. 107, no. 1, pp. 17, 1985.

- [4] P. Song, Y. Q. Yu and X. P. Zhang, "Impedance Control of Robots: An Overview," *IEEE International Conference on Cybernetics, Robotics and Control*, pp. 51-55, July 21-23, 2017.
- [5] R. J. Anderson and M. W. Spong, "Hybrid impedance control of robotic manipulators," *IEEE Journal on Robotics and Automation*, vol. 4, pp. 549-556, Oct. 1988.
- [6] B. Heinrichs, N. Sepehri and A. B. Thornton-Trump, "Position-based Impedance Control of an Industrial Hydraulic Manipulator," *IEEE Control Systems*, vol.17, pp.46-52, Feb. 1997.
- [7] J. W. Sensinger and R. F. f. Weir, "Unconstrained Impedance Control Using a Compact Series Elastic Actuator," *Proc. of 2nd IEEE/ASME International Conference on Mechatronics and Embedded Systems and Applications*, pp. 1-6, Aug. 2006.
- [8] B. Vanderborght et al., "Variable Impedance Actuators: Moving the Robots of Tomorrow," *Proc. of IEEE/RSJ International Conference on Intelligent Robots and Systems*, pp. 5454-5455, Oct. 2012.
- [9] Y. H. Tsoi and S. Q. Xie, "Impedance Control of Ankle Rehabilitation Robot," *Proc. of IEEE International Conference on Robotics and Biomimetics*, pp, 840-845, Feb. 21-26, 2009.
- [10] Y. C. Fung, *Biomechanics: Mechanical Properties of Living Tissues*, 2nd ed: Springer-Verlag New York, Inc., 1993.

Acknowledgements

This research was supported by the research fund from Northwell Health Hospital and Hofstra University.